

# **Myelin transcription factors 1 and 3 have overlapping but distinct roles in insulin secretion and survival of human $\beta$ cells**

Ruiying Hu<sup>1</sup>, Mahircan Yagan<sup>1</sup>, Yu Wang<sup>2</sup>, Xin Tong<sup>3</sup>, Teri D. Doss<sup>3</sup>, Jinhua Liu<sup>3</sup>, Yanwen Xu<sup>1,4</sup>, Alan J. Simmons<sup>1,4</sup>, Ken S. Lau<sup>1,4</sup>, Roland Stein<sup>3</sup>, Qi Liu<sup>2</sup>, and Guoqiang Gu<sup>1,\*</sup>

1, Department of Cell and Developmental Biology, Vanderbilt University School of Medicine, Nashville, TN 37232, USA.

2, Department of Biostatistics and Center for Quantitative Sciences, Vanderbilt Medical Center, Nashville, TN37232, USA.

3, Department of Molecular Physiology and Biophysics, Vanderbilt University School of Medicine, Nashville, TN 37232, USA.

4, Epithelial Biology Center, Vanderbilt Medical Center, Nashville, TN 37232, USA.

\*: Corresponding author: Guoqiang.gu@vanderbilt.edu (615)-936-3634

**Keywords:** MYT1, ST18, MYT3, stress response, obesity,  $\beta$ -cell failure, apoptosis, diabetes, insulin resistance, insulin secretion, anterior eye chambers, transplantation.

## **Highlights:**

- MYT1-KD compromises human  $\beta$ -cell survival but not insulin secretion
- MYT3-KD compromises human  $\beta$ -cell insulin secretion but not survival
- MYT3-KD compromises human  $\beta$ -cell viability in obesity
- MYT1 and MYT3 regulate overlapping but distinct sets of genes

**Short title:** MYT-TFs in human  $\beta$ -cell survival and function

## Abstract

Islet  $\beta$ -cell dysfunction, loss of identity, and death, together known as  $\beta$ -cell failure, lead to reduced insulin output and Type 2 diabetes (T2D). Understanding how  $\beta$ -cells avoid this failure holds the key to preventing or delaying the development of this disease. Here, we examine the roles of two members of the Myelin transcription factor family (including MYT1, 2, and 3) in human  $\beta$ -cells. We have reported that these factors together prevent  $\beta$ -cell failure by repressing the overactivation of stress response genes in mice and human  $\beta$ -cell lines. Single-nucleotide polymorphisms in MYT2 and MYT3 are associated with human T2D. These findings led us to examine the roles of these factors individually in primary human  $\beta$ -cells. By knocking down *MYT1* or *MYT3* separately in primary human donor islets, we show here that these TFs have distinct functions. Under normal physiological conditions, high *MYT1* expression is required for  $\beta$ -cell survival, while high *MYT3* expression is needed for glucose-stimulated insulin secretion. Under obesity-induced metabolic stress, MYT3 is also necessary for  $\beta$ -cell survival. Accordingly, these TFs regulate different genes, with MYT1-KD de-regulating several in protein translation and  $\text{Ca}^{2+}$  binding, while MYT3-KD de-regulating genes involved in mitochondria, ER, etc. These findings highlight not only the family member-specific functions of each TF but also the multilayered protective function of these factors in human  $\beta$ -cell survival under different levels of metabolic stress.

## Introduction

Type 2 diabetes (T2D) develops when endocrine islet  $\beta$ -cells cannot secrete enough insulin for whole-body glucose homeostasis.  $\beta$ -cell failure (including dysfunction, loss of identity, and/or cell death) is a significant cause of this defect (1). However, how  $\beta$ -cell failure is induced remains incompletely understood.

A major inducer of  $\beta$ -cell failure is obesity, which can induce insulin resistance in the fat, the liver, and skeletal muscle. These primary tissues take up circulating glucose under insulin stimulation (2-6). To compensate,  $\beta$ -cells increase insulin output in response to the high glucose and free fatty acid levels in circulation. However, sustained high insulin

output can exhaust the  $\beta$ -cells due to the stressor-producing nature of insulin secretion (4,7). Specifically, high levels of glucose metabolism will promote insulin biosynthesis, co-producing unfolded proinsulin in the endoplasmic reticulum (ER), that when reaching high levels induce ER stress and dysfunction (8). In addition, high glucose and free fatty acid metabolism in  $\beta$ -cells produce reactive oxygen species (ROS) and/or toxic lipid metabolites (9). These products, at high levels, cause oxidative stress and mitochondrial dysfunction while also exacerbating ER stress. Henceforth,  $\beta$ -cells activate unfolded protein response (UPR) and/or oxidative stress response (OSR) to clean up these stressor molecules (10-12). If properly controlled, the overall result of these responses is proteomic homeostasis and sustainable  $\beta$ -cell function. However, stress responses can last too long or be overly activated, compromising the production of essential  $\beta$ -cell proteins or inadvertently activating proapoptotic genes (3,13). Thus, both the inactivation and overactivation of stress responses contribute to diabetes, underscoring the importance of stress response regulation in  $\beta$ cell failure (14).

The myelin transcription factor (MYT TF) family consists of three zinc finger proteins that are primarily expressed in neuronal and endocrine cells [Myt TFs, including *Myt1* (*Nzf2*), *Myt2* (*Myt1L*, *Nzf1*), and *Myt3* (*St18*, *Nzf387*)]. They can serve as both transcriptional repressors or activators in a cell type- and context-dependent fashion, likely via the association with co-regulators SIN3 or LSD1 (15,16). Underscoring the importance of these factors for human health, single-nucleotide polymorphisms and deletion mutations in any of the three are associated with human diseases, including mental illness, cancer, and diabetes (17-22). In mice, inactivating *Myt1* alone in the mouse pancreas results in glucose intolerance and  $\beta$ -cell dysfunction without compromising  $\beta$ -cell viability and proliferation (23). In contrast, co-inactivating all three results in  $\beta$ -cell dysfunction, reduced proliferation, and death, leading to late-onset diabetes (24). Mechanistically, these mutant phenotypes appear to be caused by the de-repression of several stress response effectors, including heat shock proteins and activating transcription factors (e.g., *Atf4*) involved in UPR in the ER, cytoplasm, and mitochondria (25-28). More importantly, this mechanism appears conserved in human  $\beta$ -

cells. In this regard, we found that the protein levels and/or nuclear localization of MYT1/MYT3 were regulated by glucose and free fatty acids in human  $\beta$ -cells (24). In addition, the reduced MYT TF production correlated with human  $\beta$ -cell dysfunction during the development of T2D (24). Lastly, we showed that co-knockdown (KD) of all three factors compromised the viability of a human  $\beta$ -cell line while inducing the transcription of several stress response genes (24).

The above studies establish the Myt TFs as key regulators against cellular stress-induced  $\beta$ -cell failure. However, the specific functions of these single factors in human  $\beta$ -cells remain unknown, especially since the co-KD of these factors leads to cell death, preventing more detailed characterization of the mutant cells. This study examines the roles of MYT1 and MYT individually in primary human donor islets. We highlight the overlapping and distinct functions of these two factors.

## **Research design and methods**

### ***Lentiviral production for gene knockdown***

Lentiviral production and usage followed the protocol described in (29). Briefly, we selected four candidate shRNA sequences for either MYT1 or MYT3 based on our successful KD of these genes using a mix of these siRNAs (Huang et al., 2020). These shRNA were expressed in individual DNA constructs under the control of a U6 promoter, which also drives eGFP with a CMV promoter for successful transfection. To test the effectiveness of these shRNAs, a reporter construct was made for each shRNA by inserting the target sites of these shRNAs into the 3' end of mCherry-producing transcripts (distal to the coding region), driven by a CMV promoter (Fig. S1A). The shRNA and reporter plasmids were then co-transfected into the HEK293 cells. The ratio between eGFP and mCherry is then used as a parameter to score the effects of shRNA, which was further verified via real-time RT-PCR (Fig. S1B-G). The most effective shRNAs were verified in human EndoC- $\beta$ H3 cells (Fig. S1H, I) and used for lentivirus production.

### ***Pseudo-islets preparation for gene knockdown***



Pseudo-islet production followed the published protocol (30). Primary human donor islets were procured from IIDP. Upon receiving, a few islets were set aside to check the stimulation index (insulin secretion under 16.7 mM glucose over that under 2.8 mM). Only islets with a stimulation index higher than 2.5 (artificially set) will be used for downstream studies. Briefly, within 24 hours after receiving, islets were washed and dissociated into single cells using 0.25% trypsin at room temperature, usually taking <3 Min. The cells were washed twice with standard CMRL islet media (CMRL1066 with 10% heat-inactivated FBS, 1X antibiotics, and 1X L-glutamine). The cells were then resuspended in VPM media (50% CMRL1066 + 50% Vasculife Basal Media, 10% heat-inactivated FBS, 1X antibiotics, 0.5X Glutamax, 2.5 mM HEPES, 0.5X sodium pyruvate plus rh VEGF LifeFactor, rh EGF LifeFactor, rh FGF basic LifeFactor, rh IGF-1 LifeFactor, Ascorbic Acid LifeFactor, Hydrocortisone Hemisuccinate LifeFactor, Heparin Sulfate LifeFactor, Gentamicin/Amphotericin, L-glutamine LifeFactor B, and iCell Endothelial Cells Medium Supplement. All these factors are provided in the VEGF complete kit from MDsystems). The cells were then counted and diluted to 1,000,000 per ml with VPM. The suspension was then aliquoted into each well of a prepared Aggrewells 96-well plate at 200,000 cells per well. Then 40-50 ng of lentivirus was added and mixed well. The plate was centrifuged at 200g for 5 min and left undisturbed in a cell culture incubator for 6 days. The pseudo-islets were then recovered for downstream studies. For preparing the wells, add 100ul/well of anti-adhesive rinsing solution into Aggrewells (96-well late, Nacali #4860-900SP), Centrifuge at 1300g for 5min, Room temp, Aspirate the anti-adhesive solution.

### ***Immunofluorescence (IF) staining***

IF staining follows routine methods. Paraffin (TUNEL assays and endocrine hormone staining) or frozen (transcription factor staining) sections were used. TUNEL assays, using kits from Invitrogen, were used to monitor cell death, following the manufacturer's protocols.

Antibodies and dilution used were: rabbit anti-Pdx1 (1:5000) and guinea pig anti-Pdx1 (1:2000) (gifts from Chris Wright, Vanderbilt University School of Medicine); mouse

anti-glucagon (1:5000) (Dako); goat anti-somatostatin (1:500) (Millipore); rabbit anti-somatostatin (1:2000) (Santa Cruz); rabbit anti-PPY (1:500) (Abcam); goat anti-c-peptide (1:500) (Santa Cruz); guinea pig anti-insulin (1:1000) (Dako); rabbit anti-Myt1 (1:1000) (this lab); rat anti-Myt3 (1:1000) (this lab); rabbit anti-MafA (Novus, RRID: AB\_1503594); and chicken anti-Nkx6.1 (Developmental Studies Hybridoma Bank, F55A10). All secondary antibodies were from Jackson ImmunoResearch, with Cat# available if requested.

For imaging, slides were counter-stained with DAPI (when indicated) and imaged with laser scanning confocal microscopy (FV1000). Image J was used to quantify the data.

### ***Gene expression assays by qPCR, scRNA-seq, and bulk RNA-seq***

Real-time reverse transcription qPCR followed routine method. For shRNA inhibition tests, each well of transfected HEK293 cells was split into two samples; one sample was directly used to determine the copy numbers of transfected plasmids to normalize transfection efficiency via real-time qPCR. RNA was isolated from the other half of the transfected cells using a DNA-free RNA<sup>TM</sup> kit (Zymo Research). Between 100-200 ng total RNAs were then used for cDNA preparation using a Promega high-capacity synthesis kit. Real-time qPCR was performed utilizing the SYBR green master mix of the Bio-Rad system. For plasmid DNA determination, oligos 5'-aactttggcattgtggaagg-3'+ 5'-ggatgcagggatgatgttct-3' were used. For determining the mCherry transcript level, oligos 5'-aactttggcattgtggaagg-3'+ 5'-ggatgcagggatgatgttct-3' were used. The effects of shRNA on gene knockdown were estimated by calculating the degree of mCherry mRNA reduction, normalized against the copy numbers of the reporter plasmid.

For testing the MYT1 and MYT3 KD efficacy in freshly made pseudo-islets, RNA/cDNA prep and PCR followed the steps outlined above. GAPDH was used as a loading control. Oligos used were: GAPDH: 5'-ctttggtatcgtggaaggactc-3' and 5'-agtagaggcagggatgatgt-3'. For MYT1: 5'-ggccacatcaccgggaacta-3' and 5'-agtgggcagccatgaggttt-3'. For MYT3: 5'-ggcatgcagactctgtggct-3' and 5'-catccacagccagccattcg-3'.

For scRNA-seq, dissociated pseudo-islets with ~80-90% single cells and <5% dead cells were used for InDrop, strictly following the manufacturer's protocol. The end library was sequenced with Novaseq 6000 (Illumina), targeting 120 million reads. DropEst (31) was then used to preprocess scRNA-seq reads and to generate count matrices. Cells with low unique mapping reads (<500), low proportion of expressed genes (<100), or high proportion of mitochondrial RNAs (>10%) will be excluded (Fig. S3). Reads were normalized using UMI-filtered counts. Cell subpopulations were identified and visualized by UMAP using Seurat based on the first 30 principal components generated from the top 2000 highly variable genes (32,33). Differentially expressed genes (DEGs) between mutant and control  $\beta$ -cells were identified by Seurat at the criteria of  $|\log_2 \text{fold change}| > 0.25$  &  $\text{FDR} < 0.05$ . Database for Annotation, Visualization and Integrated Discovery (DAVID) was then used for functional clustering analysis of DEGs (34), with similar pathways or processes consolidated and presented (top 10 only). Pathways with p-values <0.05 were considered significant.

Bulk RNAseq and analysis follow that outlined in (35) for RNA preparation and sequencing. Data analyses used the workflow described in Genialis, which identifies about 60,000 transcripts (36). For downstream processing, only genes with detectable expression were used (especially for hypergeometric analysis, which needs to know the pool of genes from which candidate genes were derived). For this, we considered genes with RPKM >0.5 as a cutoff because this ensured at least an average of one RNA molecule detected in each cell (37). Pair t-tests were used to identify differentially expressed genes (DEGs). Because of the known variability of human donor islet samples, we consider p values <0.05, with a difference of 20%, statistically significant to minimize rejecting false negatives.

### ***Pseudo Islet transplantation and follow-up analysis***

Pseudo-islets were collected from Aggrewells and recovered in RPMI1640 (11 mM glucose, 10% FBS, 1X antibiotics) overnight. They were then separated into ~30 pseudo-islets/groups and transplanted into the anterior eye chambers (AECs) of NSG-DTR mice

following established protocols (38). Some of the transplants were recovered 4 weeks after transplantation for characterization. Others were recovered and studied after feeding recipient mice for three months with a high-fat diet (HFD), starting 4 weeks after transplantation.

### ***Insulin tolerance test***

Insulin tolerance tests follow standard protocol. Mice were fasted for 4 hours (starting around 8 am). Insulin Humalog was then injected at 0.5 Units/kg. Blood glucose levels were then read via the tail vein at 0, 15, 30, 45, and 60 min after the injection.

### ***Statistical analysis***

The students' *t*-test was used to make pairwise comparisons at single time points or paired genotypes. Two-way ANOVA was used to compare multiple groups of data points. Hypergeometric analyses were used to assess the level of enrichment between lists of genes. A *p*-value  $\leq$  0.05 was considered significant.

### ***Data Accessibility and request for materials***

The RNAseq data will be available in the Gene Expression Omnibus (GEO) database. Further requests for resources and reagents should be directed to and will be fulfilled by the Lead Contact [Guoqiang.gu@vanderbilt.edu](mailto:Guoqiang.gu@vanderbilt.edu) (615-936-3634).

## **Results**

### **Establishing effective MYT1 and MYT3 knockdown (KD) in human islet $\beta$ cells**

We have shown that MYT1, MYT2, and MYT3 are differentially regulated by high glucose and free fatty acids in human  $\beta$ -cells, physiological inducers of  $\beta$ -cell failure. This led us to examine the roles of these factors individually. We focused on MYT1 and MYT3 because these paralogs, but not MYT2, are regulated by high glucose or free fatty acid treatment in human donor islets (24). For this goal, we used lentivirus-driven shRNA

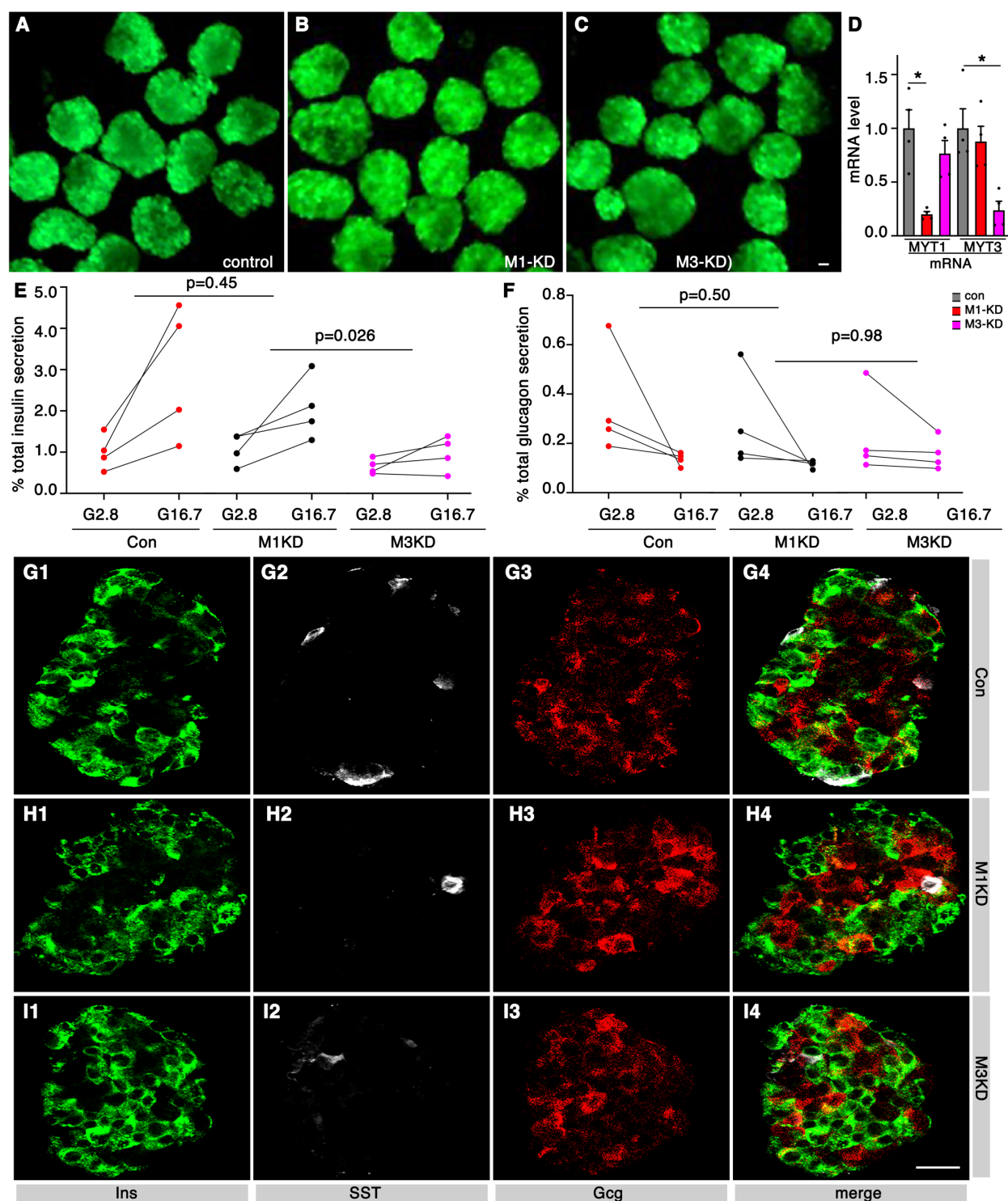
delivery for gene KD, which could effectively reduce the expression of target genes, as we showed before (29).

By comparing the gene knockdown effects of several shRNAs (see Materials and Methods), we identified two that can effectively target the *MYT1* or *MYT3* mRNAs, respectively (Fig. S1A-G). Lentiviral delivery (marked with eGFP expression) of these shRNAs could efficiently and specifically reduce the MYT1 or MYT3 protein levels compared with scrambled shRNA controls, respectively, in EndoC- $\beta$ H3 cells (Fig. S1H, I). These constructs were therefore used to KD MYT1 or MYT3 in primary human islet cells. All studies used A lentiviral construct expressing a scrambled shRNA and eGFP as a control.

### **Knockdown of MYT3 but not MYT1 impaired human $\beta$ -cell glucose-stimulated insulin secretion (GSIS)**

Primary human islets from four healthy donors were dissociated into single cells, infected with shRNA-producing lentivirus, and made into pseudo-islets (Fig. 1A-C). This resulted in 70-80% KD of both genes six days after viral infection (Fig. 1D). MYT1-KD did not change the GSIS of pseudo-islets compared with controls (Fig. 1E). In contrast, MYT3-KD resulted in a significant reduction in GSIS (Fig. 1E). These findings suggest that high levels of MYT3 but not MYT1 is required for GSIS in human primary  $\beta$ -cells. Note that there was no difference in glucagon secretion in control, MYT1-KD, and MYT3-KD pseudo-islets (Fig. 1F). We therefore focused on  $\beta$  cells from now on.

**Fig. 1. Knock-down of MYT3, but not MYT1, impaired GSIS of primary human  $\beta$  cells.**



Procured primary human islets, after quality check, were dissociated into single cells, infected with lentivirus that drives the expression of control, MYT1(M1)-targeting, or MYT3 (M3)-targeting shRNAs, and made into pseudo-islets. They were allowed to recover overnight in fresh media and tested for GSIS. (A-C) Representative pseudo-islets, with eGFP as a marker of lentivirus infection. (D) RT-PCR assays showing MYT1 or MYT3 KD levels in one pseudo-islet batch. Shown are mean + SEM. \*:  $p < 0.02$ , calculated via t-test (with two-tailed type two errors). (E, F) Secretion assays of insulin (E) or glucagon (F) in response to



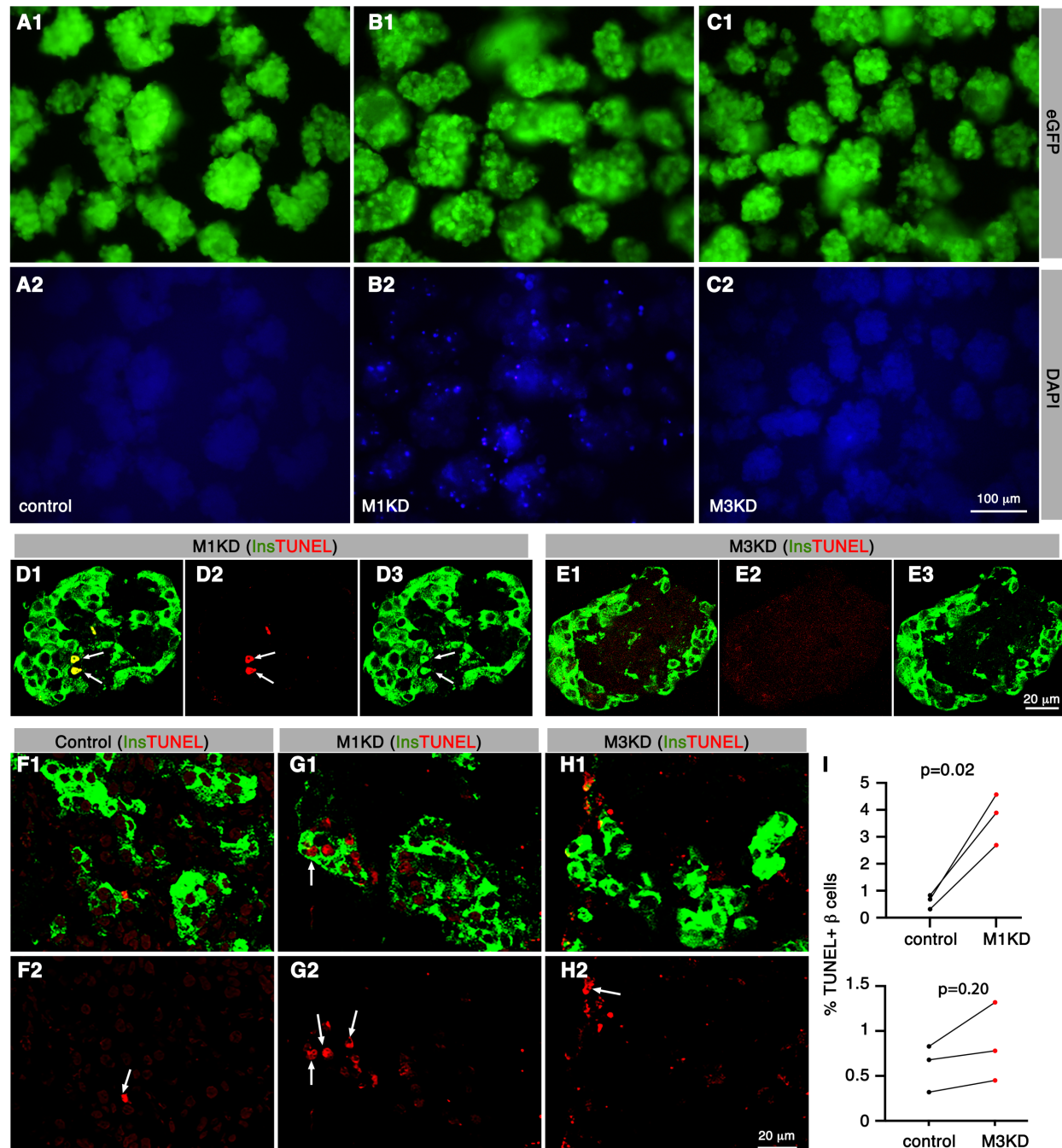
G2.8 or G16.7. Each dot represents assays of one batch of pseudo-islets, with 3 or 4 secretion assays. P values are from two-way ANOVA. (G-I) Hormone expression assays in newly-produced pseudo-islets. Note that image panels from the same field of view were marked with the same capital letter (followed by a number to indicate different channels). Scale bars = 20  $\mu$ m.

Because single *Myt1* knockout in mice leads to the production of multi-hormone<sup>+</sup> cells, we also examined if MYT1- or MYT3-KD induced such defects. We did not observe a significant number of cells that co-expressed insulin with glucagon or somatostatin (SST) (Fig. 1G-I), nor pancreatic polypeptide (PPY) (Fig. S2). These findings suggest that high MYT1 or MYT3 activity is dispensable for preventing the activation of other hormones in human  $\beta$ -cells. We next examined cell death in these pseudo-islets.

### **MYT1-KD but not MYT3-KD induces human $\beta$ -cell death in pseudo-islets *in vitro***

Because co-KD of all three MYT TFs in EndoC- $\beta$ H1 cells induces cell death (24). We examined whether knocking down each induces primary  $\beta$ -cell death. Freshly prepared pseudo-islets were stained briefly with DAPI, expecting DAPI to pass through the plasma membrane of dead cells to label their nuclei. MYT1-KD but not MYT3-KD pseudo-islets contained significant DAPI<sup>+</sup> cells (Fig. 2A-C). TUNEL assays confirmed that some dead cells expressed insulin (Fig. 2D, E).

**Fig. 2. Knock-down of MYT1, but not MYT3, caused the death of primary human  $\beta$  cells *in vitro* and *in vivo* under normal physiology.**



Freshly made pseudo-islets, with control, MYT1(M1)-KD, or MYT3 (M3)-KD, were stained with DAPI to visualize dead cells. They were also examined for cell death with TUNEL assays before or 4 weeks after transplantation into the AEC of mice. (A-C) DAPI staining to show the presence of DAPI+ cells without any treatment. Note that image panels from the same field of view were marked with the same capital letter (followed by a number to indicate different channels). Also note that panels A2 and C2 were purposely over-exposed to show the cells. (D-E) TUNEL staining of freshly made pseudo-islets. White arrows pointed at two dead cells with Insulin-signals. (F-I) TUNEL assays and quantification of dead β cells 4 weeks after pseudo-islets were transplanted into AEC of mice. White arrows pointed at several dead insulin+ cells. In I, each dot represents results from one batch of islets, with each batch transplanted into at least three mice. P values were from paired t-tests (with data from the same donor pair).

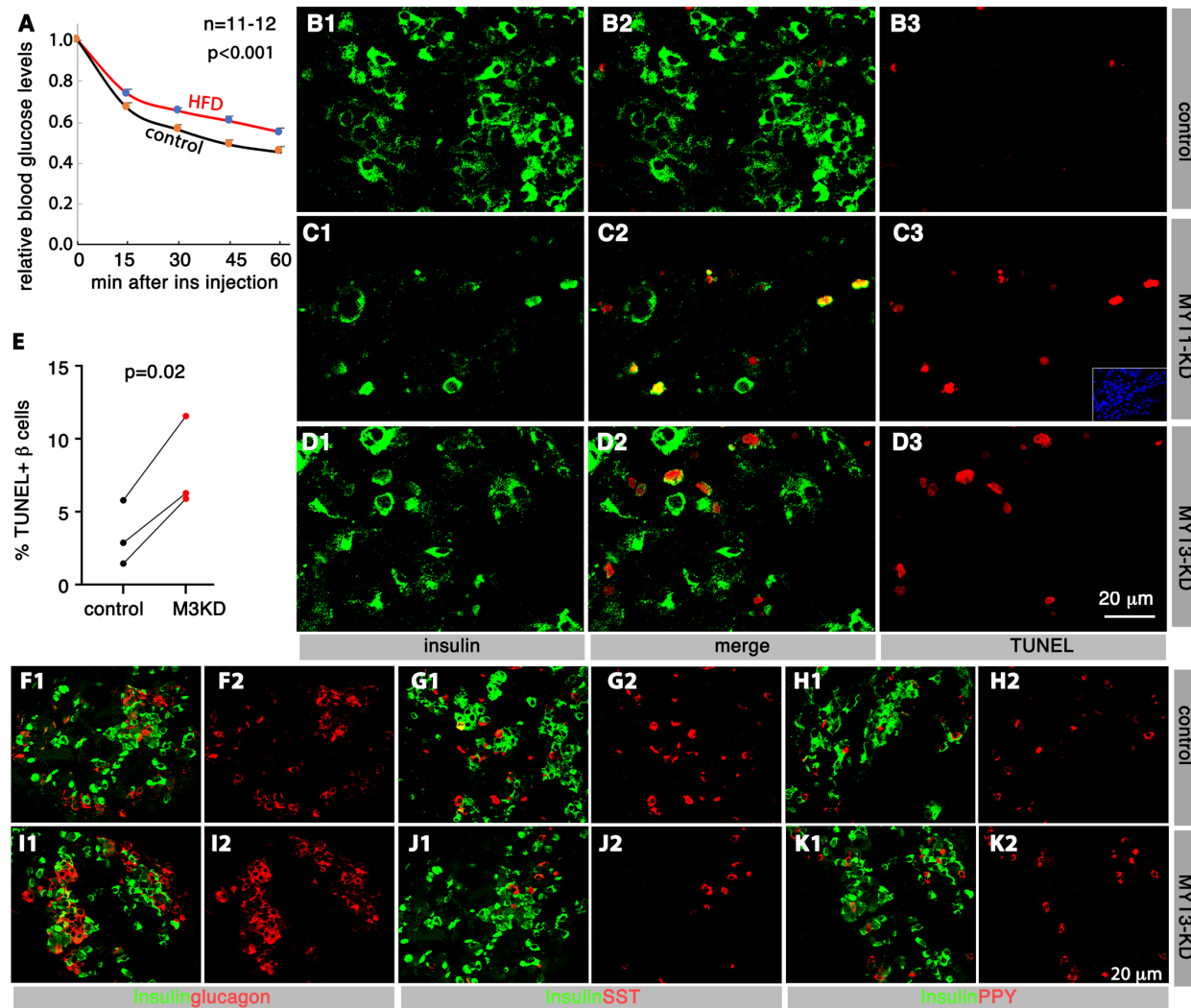


Because human  $\beta$ -cell death detected *in vitro* was sometimes not shown *in vivo* (39), we examined how  $\beta$  cells with MYT1- or MYT3-KD behaved *in vivo*. Pseudo-islets were transplanted into the anterior eye chambers (AECs) of NSG-DTR. The transplants were recovered four weeks later for cell death assays (Fig. 2F-H). In all three donor samples tested, we found significantly more  $\beta$ -cell death upon MYT1-KD but not upon MYT3-KD compared with controls (Fig. 2I). These results suggest that MYT1 but not MYT3 is required for human  $\beta$ -cell survival under normal physiological conditions. Note that one batch of islets had a very low yield of pseudo-islets and was not tested for cell death *in vivo*.

### **MYT3-KD renders human $\beta$ -cells vulnerable to obesity-induced death**

Because we have recently shown that mouse  $\beta$ -cells with *Myt-TF* deficiency are vulnerable to obesity-induced  $\beta$ -cell death, we examined how human  $\beta$  cells with MYT1- or MYT3-Kd respond to obesity. Mice transplanted with control, MYT1-KD, or MYT3-KD pseudo-islets were fed with HFD for three months, starting 4 weeks after transplantation. This induced significant insulin resistance in mice compared with controls (Fig. 3A). The transplants were then recovered and assayed for  $\beta$ -cell death. Consistent with the requirement of MYT1 for  $\beta$ -cell survival, very few  $\beta$  cells were detected in MYT1-Kd samples after three months of HFD challenge (Fig. 3B, C) (making it a challenge for quantification). We, therefore, focus on examining the  $\beta$  cells with MYT3-Kd.

**Fig. 3. MYT3-KD renders primary human  $\beta$  cells vulnerable to high-fat-diet-induced cell death.**



Four weeks after the operation, mice transplanted with manipulated pseudo-islets were fed with HFD for three months. Pseudo-islets were then recovered for characterization. (A) Insulin tolerance test to show the HFD-induced insulin resistance in recipient mice. The starting blood glucose of each animal was normalized to “1”. The P value is from two-way ANOVA. (B-E) TUNEL-assays of recovered transplants. Image panels from the same field of view were marked with the same capital letter (followed by a number to indicate different channels). Inset in C3 showed a DAPI staining in processed sections to visualize all nuclei. In E, each dot represents data from one islet batch, which included at least three transplanted mice. P is from paired t-tests. (F-K) IF showing the hormone co-expression status (between insulin and others) in recovered transplants.

Significantly more β-cell death was detected in transplants with MYT3-KD compared with controls three months after the HFD challenge (Fig. 3D, E). Under this condition, we did not detect significant numbers of insulin-expressing cells activating the expression of other hormones, including glucagon, SST, and PPY (Fig. 3F-K). These results suggest that, unlike total *Myt* TF inactivation in mice, MYT3-KD in human β cells

did not induce spurious activation of other islet hormones, a feature of  $\beta$ -cell transdifferentiation.

These combined findings suggest that MYT1 and MYT3 have overlapping but different functions in human  $\beta$  cells. The former is primarily required for protecting cell viability, while the latter is for secretory function. Yet, at high-stress levels, both are needed for  $\beta$ cell viability. We next examined the gene expression changes induced by the KD of these factors.

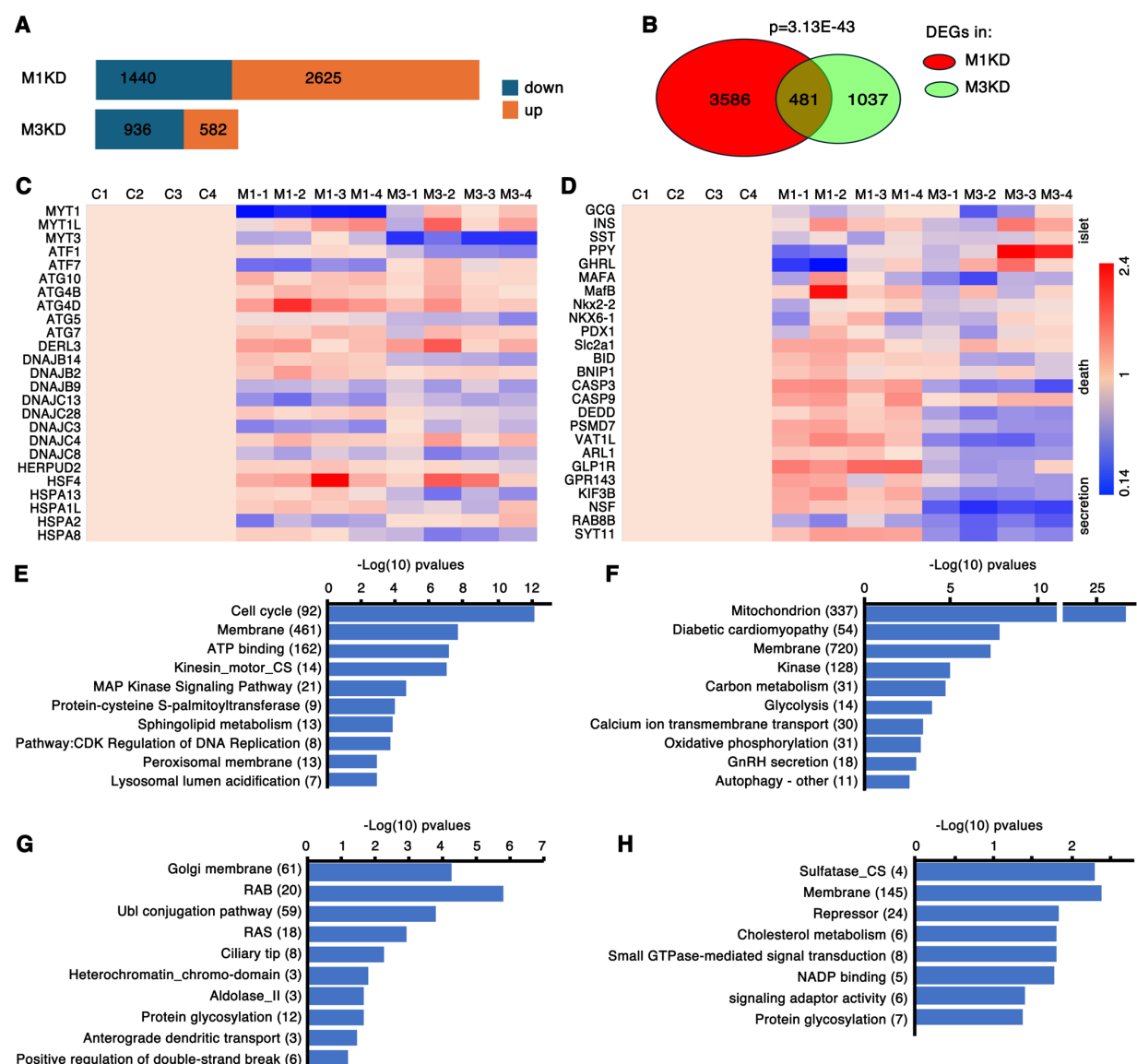
### **MYT1 and MYT3 have overlapping but different gene regulatory networks in pseudo-islets**

We utilized RNAseq to examine the effect of MYT1 or MYT3 KD on gene expression in human islet cells. For this goal, we used the pseudo-islets before their transplantation into mice, which we envision to capture the gene expression changes before cells experience physiological stress from recipient mice. Both RNAseq from intact pseudo-islets and scRNA-seq from dissociated pseudo-islet cells were performed. The former was expected to capture MYT TF-regulated genes in all islet cells, while the latter would allow focused studies of  $\beta$  cells.

Bulk RNAseq from four donor islet batches identified 4,065 or 1,518 differentially expressed genes (DEGs) between control and MYT1-KD or MYT3-KD pseudo-islets, respectively (Fig. 4A) (Table S1). Consistent with the similar functions of the two paralogs, MYT1-KD and MYT3-KD share 509 DEGs (Table S1), a 4.55 folds enrichment over random overlapping among 23,000 genes with detectable expression (at least one mRNA in each cell) (Fig. 4B) ( $p=8.01e-200$ , hypergeometric analysis). Intriguingly, we found several stress response-related genes were dysregulated with either MYT1- or MYT3-KD or both conditions (Fig. 4C), consistent with the known roles of MYT TFs in stress response. These genes include several activating transcription factor genes (*ATF1*, *ATF7*) that are involved in stress response (40,41), ATG genes that are involved in autophagy (42), and two families of heat shock-proteins (DNAJs and HSPs) (Fig. 4C) (24). Note that

consistent with the specificity of shRNA-based gene KD, we only detected significant down-regulation of MYT1 or MYT3 when their respective shRNA was used (Fig. 4C).

**Fig. 4. Human islet cells with MYT1 or MYT3 KD deregulates overlapping but distinct genes.**



Freshly prepared pseudo-islets were directly used for total RNA prep and sequencing. (A) The numbers of genes that were down- or upregulated with M1KD or M3KD in total pseudo-islets. (B) The numbers of common and specific genes affected by MYT1 or MYT3 KD. (C, D) Heat maps of a few MYT1- or MYT3-regulated genes in four pseudo-islet duplicates, focusing on those involved in stress (C) or function (D). In sample annotations on the top, C1-C4 refers to the four independent controls. M1-1 to M1-4 are the four samples with MYT1-KD. M3-1 to M3-4 are the four samples with MYT3-KD. (E, F) Pathways deregulated in M1KD human pseudo-islets, composed by down- or up-regulated (F) genes in mutants. (G, H)

Pathways deregulated in M3KD human pseudo-islets, composed of down- (G) or up-regulated (H) genes in mutants.

We performed a supervised DEG analysis to understand why *MYT1* and *MYT3* have different functions in  $\beta$ -cell survival and secretion. This comparison identified several DEGs that are associated with cell death and vesicular biosynthesis/secretion (Fig. 4D). Notably, *BID* (43), *CASP3* (44), *DEDD* (45), and *PSMD7* (46), all known to regulate cell death, were upregulated in MYT1-KD pseudo-islets but down-regulated in MYT3-KD samples (Fig. 4D). Along a similar line, the expression of *ARL1* (47), *GLP1R* (48), *KIF3B* (49), *NSF* (50), *RAB8B* (51), and *SYT11* (52), all known to regulate vesicular production or secretion, were also upregulated in the MYT1-KD but not MYT3-KD cells (Fig. 4D).

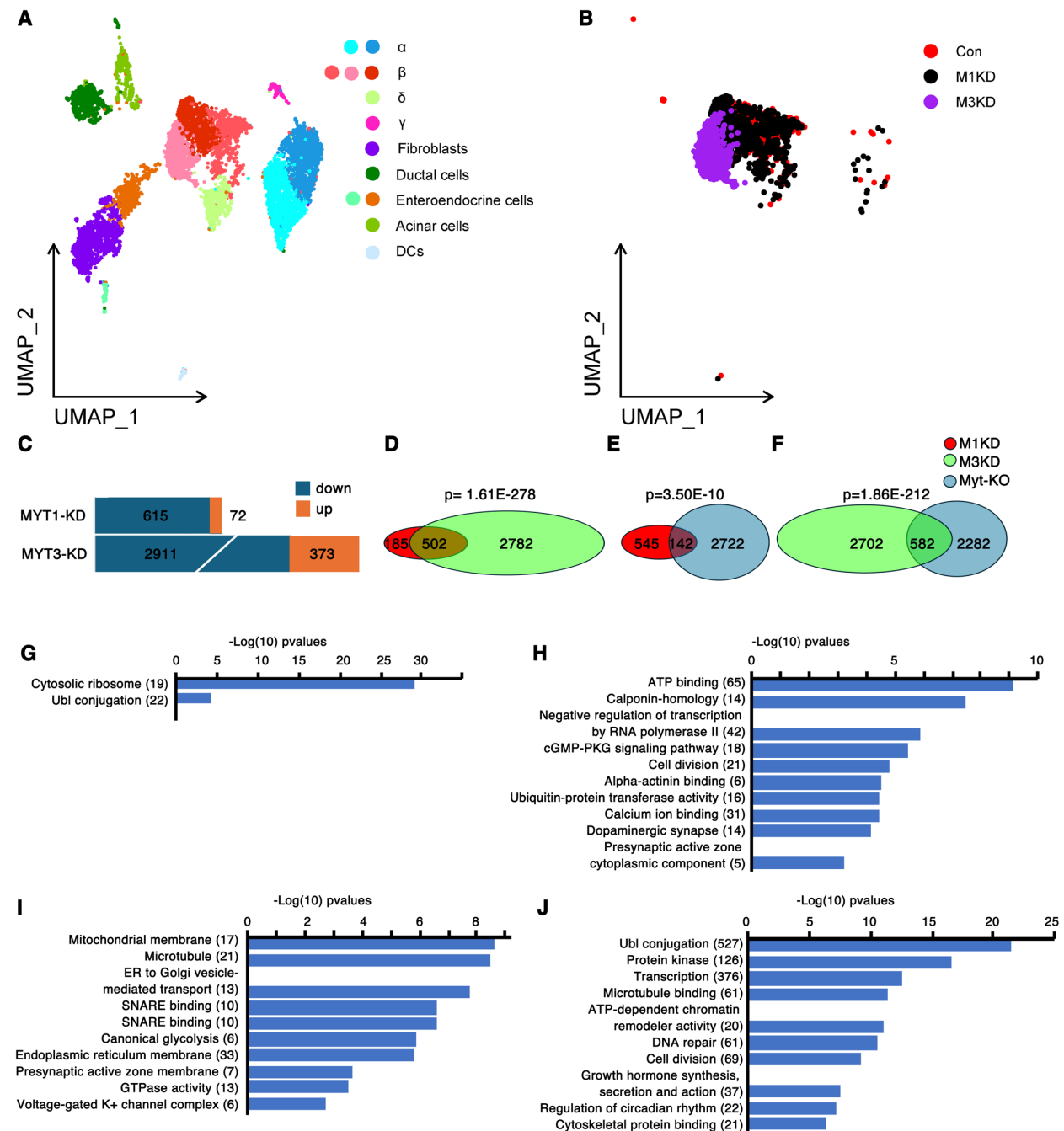
Next, we examined the up-regulated or down-regulated processes in the MYT1-KD or MYT3-KD pseudo-islets. The down-regulated pathways in MYT1-KD samples include those controlling *Cell cycle*, *Membrane*, *Kinesin motor*, *MAP kinase signaling*, etc. (Fig. 4E), while up-regulated pathways include *Mitochondrion*, *membrane*, *kinase*, *carbon metabolism*, *glycolysis*, *Ca<sup>2+</sup> transport*, etc. (Fig. 4F). In contrast, MYT3-KD down-regulated genes mainly regulate *Golgi*, *G proteins*, and *Ubl conjugation pathway* but upregulate those involved in *Sulfatase-CS*, *membrane*, *repressor*, *cholesterol metabolism*, etc. (Fig. 4G, H).

### ScRNA-seq revealed DEGs upon MYT1- or MYT3-KD specifically in $\beta$ -cell

The bulk RNAseq gave us global views of gene expression from pseudo-islets. To understand the mechanism used by Myt TFs in regulating human  $\beta$ -cells, scRNA-seq was used to examine gene expression with MYT1- or MYT3-KD. High-quality sequencing data were obtained from one batch of pseudo-islets, shown by the significant reduction of *MYT3* transcripts in the MYT3-KD samples (Table S1). All the major islet cell types in pseudo-islets ( $\alpha$ ,  $\beta$ ,  $\delta$ , and  $\gamma$ ) and non-islet cells were identified (Fig. 5A). Notably, there was a clear separation of control and MYT3-KD  $\beta$  cells but not between control and MYT1-KD  $\beta$  cells (Fig. 5B). Corresponding to this observation, we found 687 DEGs between control and MYT1-KD samples and 3,284 DEGs between the control and MYT3-KD samples (Fig. 5C) (Table S1). The lack of separation between control and MYT1-KD cells

and the lower number of DEGs between control and MYT1-KD  $\beta$  cells (compared with that between control and MYT3-KD cells) likely resulted from the death of the  $\beta$  cells with high levels of MYT1-KD.

**Fig. 5. Human MYT1 or MYT3 KD in  $\beta$ -cells deregulate similar but distinct gene networks.**





Freshly prepared pseudo-islets were dissociated and used for InDrop scRNA-seq. (A, B) UMAPs showing the separation of cells in pseudo-islets, including all cells (A) or  $\beta$  cells only (B). (C) The numbers of genes that were down- or upregulated with M1KD or M3KD. (D) The common and specific gene sets regulated by MYT1 or MYT3 are in human  $\beta$  cells. (E, F) Overlap of genes regulated by human MYT1 or MYT3 with that regulated by all Myt TFs in mouse  $\beta$  cells, respectively. (G, H) Pathways deregulated in M1KD human  $\beta$  cells either up- (G) or down-regulated in mutants. (I, J) Pathways deregulated in M3KD human pseudo-islets, composed by up- (I) or down-regulated (J) genes in mutants.

With the  $\beta$ -cell specific gene expression data, we explored whether the MYT TFs regulate similar gene networks amongst the different family members and between species. We found 502 DEGs were shared between those deregulated by MYT1-KD or MYT3-KD, respectively, a 5.1-fold enrichment over random overlap between islet cell-expressed genes ( $p=1.61E-278$ , hypergeometric assays) (Fig. 5D) (Table S1). We also examined whether MYT TFs regulate similar sets of genes in human and mouse  $\beta$  cells, taking advantage of the MYT-TF-dependent genes in newly born mouse  $\beta$  cells (24). We found 142 of the MYT1-KD-affected human genes were altered in Myt TF-KO mouse  $\beta$  cells, a 1.7 fold enrichment over random overlap ( $p=3.50E-10$ , hypergeometric assays) (Fig. 5E) (Table S1). Similarly, 582 of the MYT3-KD-affected genes were altered in Myt TF-KO mouse  $\beta$  cells, a 1.4 fold enrichment over random overlapping ( $p=1.86E-212$ , hypergeometric assays) (Fig. 5F) (Table S1). These results support the conserved functions of Myt TFs in mouse and human cells and the similar-but-divergent functions of MYT1 and MYT3 in human  $\beta$  cells.

We last examined the pathways affected by MYT1- or MYT3-KD in  $\beta$  cells. MYT1-KD upregulated two main processes, *cytosolic ribosome* and *Ubl conjugation* (Fig. 5G), while down-regulating processes such as *ATP binding*, *cell division*, *Ca<sup>2+</sup> binding*, and synapse-related processes (Fig. 5H). In contrast, MYT3-KD upregulated processes such as *mitochondrial membrane*, *microtubule*, *ER to Golgi trafficking*, *SNARE binding*, *glycolysis*, *ER membrane*, *K<sup>+</sup> channels*, etc. MYT3-KD also down-regulates processes such as *Ubl (ubiquitin) conjugation*, *protein kinases*, *overall transcription*, *microtubule*, etc. These processes may contribute to  $\beta$ -cell function by mediating stress responses (via, e.g., the Ubl-related process), Ca<sup>2+</sup> handling (via channel activities), and secretion (microtubule mediated transport, Ca<sup>2+</sup> influx via channel proteins, etc.). Notably, these  $\beta$ -

cell specific pathways also differ from those of the entire cell populations from pseudo-islets, suggesting that the MYT TFs may regulate different processes in different cell types.

## Discussion

Genetic predisposition and non-genetic factors work together to induce T2D in human subjects. Hundreds of genetic loci have been associated with this disease (53), while obesity is shown as the most significant risk factor for this disease. Yet, how these factors are integrated to induce T2D remains incompletely understood. Here, we examine how two of the three *MYT TF* gene family members (*MYT1* and *MYT3*) regulate primary human  $\beta$ -cell failure, the hallmark of T2D, under normal physiology and obesity-related stress. We show that despite their similar biochemical activities and physiological roles in cell culture and mouse  $\beta$  cells (24,54-57), these two factors are differentially involved in human  $\beta$ -cell secretory function and survival in a stress-dependent manner. These new findings and the association between MYT3 SNPs and human T2D highlight the graded  $\beta$ -cell protection by these MYT TFs under progressively more severe workloads, i.e., with MYT1 needed under all conditions and MYT3 under higher stress levels.

Our recent studies in mice have suggested that the MYT TFs can serve as an integrator of genetic and obesity-related factors to prevent mouse  $\beta$ -cell failure (24,27,58). The anti-correlation between MYT TF levels and human  $\beta$ -cell function during T2D development also supports the importance of the MYT TFs in human  $\beta$  cells. By knocking down MYT1 or MYT3 in human islet cells, we showed that MYT1-KD did not impact  $\beta$ -cell GSIS but led to  $\beta$ -cell apoptosis under normal physiology. In contrast, MYT3-KD compromised GSIS but did not impact cell viability under normal physiology. Intriguingly, MYT3-KD predisposed human  $\beta$  cells to obesity-induced death as xenotransplants. Corresponding to these similar yet different biological functions, we show that MYT1 and MYT3 regulate overlapping but distinct sets of genes. These results suggest that despite the high degree of similarity between these protein sequences and their similar biochemical activities (54,55), they provide complementing biological activities to ensure



$\beta$ -cell function under a variety of physiological stresses. These different activities could result from the various DNA-binding affinities or different associations with transcriptional co-regulators that dictate their downstream functions, topics to be explored in the future (15).

Our findings also highlight the species-specific roles of these factors in  $\beta$  cells. Unlike in human cells, *Myt1* inactivation in mouse islets caused  $\beta$ -cell dysfunction but did not affect  $\beta$ -cell survival (23). Similarly, although both MYT3-KD in human  $\beta$  cells and *Myt3-KO* in mouse  $\beta$  cells reduced  $\beta$ -cell GSIS but not cell viability under normal physiology (Hu and Gu, in preparation), the MYT3-KD-predisposed human  $\beta$ -cell death was not detected in *Myt3-KO* mouse cells (Hu and Gu, in preparation). In addition, although multi-hormone expressing islet cells were observed in *Myt1*-single and *MYT TF*-triple mutant mouse  $\beta$  cells, a property of transdifferentiating cells, they are not induced by MYT1- or MYT3-KD. These findings highlight the partially conserved nature of MYT-TF function in mouse and human  $\beta$ -cells.

There are several issues that we cannot address in these studies. First, we do not know whether the KD phenotypes reflect that of complete *MYT* inactivation. To this end, the gene KD setting is more likely to reflect the MYT activity change during T2D development (with reduced but not eliminated MYT TF expression) (24). It is unclear if such models (with <85% reduction) can reveal the full extent of molecular changes underlying  $\beta$ -cell dysfunction or apoptosis. Second, due to the scarcity of human donor islets, we have not tested how the co-presence of high glucose and free fatty acids impacts the manipulated  $\beta$  cells. Third, for a similar reason as above, we have not tested the effect of MYT2-KD in primary human  $\beta$  cells. Thus, it is unclear whether its activity may be differentially affected by the lack of MYT1 or MYT3 to contribute to the differentially observed phenotypes.

# Acknowledgment

## ***Author contributions***

RH, MY, XT, and GG did human islet picking, pseudo-islet production, GSIS, IF assays, and imaging. RH performed ITT. TD performed pseudo-islet transplantation. JL helped with viral production and pseudo-islet growth. YW and QL analyzed scRNA-seq data. YX, AJS, and KSL performed scRNA-seq using InDrop. RS and GG conceptualized the study. All authors participated in manuscript writing/proofing.

## ***Funding***

**This study is supported by NIDDK grants (DK125696 and DK128710 for GG, DK103831, and CA095103 for KSL, AB, and AJS).** The imaging facility used is funded by (CA68485, DK20593, DK58404, DK59637, and EY08126).

## ***Guarantor Statement***

GG is the guarantor of the study, with full access to and takes responsibility for the integrity of the data and the accuracy of the data analysis.

## ***Conflict of interest***

The authors declare no conflict of interest.

## ***Previous presentation information***

The work has not been presented anywhere.

## References cited

1. Wysham C, Shubbrook J. Beta-cell failure in type 2 diabetes: mechanisms, markers, and clinical implications. *Postgrad Med*. 2020;132(8):676-686.
2. Vilas-Boas EA, Almeida DC, Roma LP, Ortis F, Carpinelli AR. Lipotoxicity and beta-Cell Failure in Type 2 Diabetes: Oxidative Stress Linked to NADPH Oxidase and ER Stress. *Cells*. 2021;10(12).
3. Sharma RB, Landa-Galvan HV, Alonso LC. Living Dangerously: Protective and Harmful ER Stress Responses in Pancreatic beta-Cells. *Diabetes*. 2021;70(11):2431-2443.
4. Shrestha N, De Franco E, Arvan P, Cnop M. Pathological beta-Cell Endoplasmic Reticulum Stress in Type 2 Diabetes: Current Evidence. *Front Endocrinol (Lausanne)*. 2021;12:650158.
5. Kaneto H, Kimura T, Shimoda M, Obata A, Sanada J, Fushimi Y, Matsuoka TA, Kaku K. Molecular Mechanism of Pancreatic beta-Cell Failure in Type 2 Diabetes Mellitus. *Biomedicines*. 2022;10(4).
6. Efrat S. Beta-Cell Dedifferentiation in Type 2 Diabetes: Concise Review. *Stem Cells*. 2019;37(10):1267-1272.
7. Kulkarni A, Muralidharan C, May SC, Tersey SA, Mirmira RG. Inside the beta Cell: Molecular Stress Response Pathways in Diabetes Pathogenesis. *Endocrinology*. 2022;164(1).
8. Yong J, Johnson JD, Arvan P, Han J, Kaufman RJ. Therapeutic opportunities for pancreatic beta-cell ER stress in diabetes mellitus. *Nat Rev Endocrinol*. 2021;17(8):455-467.
9. Gonzalez P, Lozano P, Ros G, Solano F. Hyperglycemia and Oxidative Stress: An Integral, Updated and Critical Overview of Their Metabolic Interconnections. *Int J Mol Sci*. 2023;24(11).
10. Guo S, Dai C, Guo M, Taylor B, Harmon JS, Sander M, Robertson RP, Powers AC, Stein R. Inactivation of specific beta cell transcription factors in type 2 diabetes. *J Clin Invest*. 2013;123(8):3305-3316.
11. Scheuner D, Kaufman RJ. The unfolded protein response: a pathway that links insulin demand with beta-cell failure and diabetes. *Endocr Rev*. 2008;29(3):317-333.
12. Eguchi N, Vaziri ND, Dafoe DC, Ichii H. The Role of Oxidative Stress in Pancreatic beta Cell Dysfunction in Diabetes. *Int J Mol Sci*. 2021;22(4).
13. Yong J, Parekh VS, Reilly SM, Nayak J, Chen Z, Lebeaupin C, Jang I, Zhang J, Prakash TP, Sun H, Murray S, Guo S, Ayala JE, Satin LS, Saltiel AR, Kaufman RJ. Chop/Ddit3 depletion in beta cells alleviates ER stress and corrects hepatic steatosis in mice. *Sci Transl Med*. 2021;13(604).
14. Herbert TP, Laybutt DR. A Reevaluation of the Role of the Unfolded Protein Response in Islet Dysfunction: Maladaptation or a Failure to Adapt? *Diabetes*. 2016;65(6):1472-1480.
15. Yang X, Graff SM, Heiser CN, Ho KH, Chen B, Simmons AJ, Southard-Smith AN, David G, Jacobson DA, Kaverina I, Wright CVE, Lau KS, Gu G. Coregulator Sin3a Promotes Postnatal Murine beta-Cell Fitness by Regulating Genes in Ca(2+) Homeostasis, Cell Survival, Vesicle Biosynthesis, Glucose Metabolism, and Stress Response. *Diabetes*. 2020;69(6):1219-1231.

16. Yokoyama A, Igarashi K, Sato T, Takagi K, Otsuka IM, Shishido Y, Baba T, Ito R, Kanno J, sOhkawa Y, Morohashi K, Sugawara A. Identification of myelin transcription factor 1 (MyT1) as a subunit of the neural cell type-specific lysine-specific demethylase 1 (LSD1) complex. *J Biol Chem*. 2014;289(26):18152-18162.
17. Alaraudanjoki VK, Koivisto S, Pesonen P, Mannikko M, Leinonen J, Tjaderhane L, Laitala ML, Lussi A, Anttonen VA. Genome-Wide Association Study of Erosive Tooth Wear in a Finnish Cohort. *Caries Res*. 2018;53(1):49-59.
18. Blanchet P, Bebin M, Bruet S, Cooper GM, Thompson ML, Duban-Bedu B, Gerard B, Piton A, Suckno S, Deshpande C, Clowes V, Vogt J, Turnpenny P, Williamson MP, Alembik Y, Clinical Sequencing Exploratory Research Study C, Deciphering Developmental Disorders C, Glasgow E, McNeill A. MYT1L mutations cause intellectual disability and variable obesity by dysregulating gene expression and development of the neuroendocrine hypothalamus. *PLoS Genet*. 2017;13(8):e1006957.
19. Doco-Fenzy M, Leroy C, Schneider A, Petit F, Delrue MA, Andrieux J, Perrin-Sabourin L, Landais E, Aboura A, Puechberty J, Girard M, Tournaire M, Sanchez E, Rooryck C, Ameil A, Goossens M, Jonveaux P, Lefort G, Taine L, Cailley D, Gaillard D, Leheup B, Sarda P, Genevieve D. Early-onset obesity and paternal 2pter deletion encompassing the ACP1, TMEM18, and MYT1L genes. *Eur J Hum Genet*. 2014;22(4):471-479.
20. Kroepfl T, Petek E, Schwarzbraun T, Kroisel PM, Plecko B. Mental retardation in a girl with a subtelomeric deletion on chromosome 20q and complete deletion of the myelin transcription factor 1 gene (MYT1). *Clin Genet*. 2008;73(5):492-495.
21. Vodo D, Sarig O, Geller S, Ben-Asher E, Olender T, Bochner R, Goldberg I, Nosgorodsky J, Alkelai A, Tatarsky P, Peled A, Baum S, Barzilai A, Ibrahim SM, Zillikens D, Lancet D, Sprecher E. Identification of a Functional Risk Variant for Pemphigus Vulgaris in the ST18 Gene. *PLoS Genet*. 2016;12(5):e1006008.
22. Khor CC, Do T, Jia H, Nakano M, George R, Abu-Amero K, Duvesh R, Chen LJ, Li Z, Nongpiur ME, Perera SA, Qiao C, Wong HT, Sakai H, Barbosa de Melo M, Lee MC, Chan AS, Azhany Y, Dao TL, Ikeda Y, Perez-Grossmann RA, Zarnowski T, Day AC, Jonas JB, Tam PO, Tran TA, Ayub H, Akhtar F, Micheal S, Chew PT, Aljasim LA, Dada T, Luu TT, Awadalla MS, Kitnarong N, Wanichwecharungruang B, Aung YY, Mohamed-Noor J, Vijayan S, Sarangapani S, Husain R, Jap A, Baskaran M, Goh D, Su DH, Wang H, Yong VK, Yip LW, Trinh TB, Makornwattana M, Nguyen TT, Leuenberger EU, Park KH, Wiyogo WA, Kumar RS, Tello C, Kurimoto Y, Thapa SS, Pathanapitoon K, Salmon JF, Sohn YH, Fea A, Ozaki M, Lai JS, Tantisevi V, Khaing CC, Mizoguchi T, Nakano S, Kim CY, Tang G, Fan S, Wu R, Meng H, Nguyen TT, Tran TD, Ueno M, Martinez JM, Ramli N, Aung YM, Reyes RD, Vernon SA, Fang SK, Xie Z, Chen XY, Foo JN, Sim KS, Wong TT, Quek DT, Venkatesh R, Kavitha S, Krishnadas SR, Soumitra N, Shantha B, Lim BA, Ogle J, de Vasconcellos JP, Costa VP, Abe RY, de Souza BB, Sng CC, Aquino MC, Kosior-Jarecka E, Fong GB, Tamanaja VC, Fujita R, Jiang Y, Waseem N, Low S, Pham HN, Al-Shahwan S, Craven ER, Khan MI, Dada R, Mohanty K, Faiq MA, Hewitt AW, Burdon KP, Gan EH, Prutthipongsit A, Patthanathamrongkasem T, Catacutan MA, Felarca IR, Liao CS, Rusmayani E, Istiantoro VW, Consolandi G, Pignata G, Lavia C, Rojanapongpun P, Mangkornkanokpong L, Chansangpetch S, Chan JC, Choy BN, Shum JW, Than HM, Oo KT, Han AT, Yong VH, Ng XY, Goh SR, Chong YF, Hibberd ML, Seielstad M, Png E, Dunstan SJ, Chau NV, Bei J, Zeng

- YX, Karkey A, Basnyat B, Pasutto F, Paoli D, Frezzotti P, Wang JJ, Mitchell P, Fingert JH, Allingham RR, Hauser MA, Lim ST, Chew SH, Ebstein RP, Sakuntabhai A, Park KH, Ahn J, Boland G, Snippe H, Stead R, Quino R, Zaw SN, Lukasik U, Shetty R, Zahari M, Bae HW, Oo NL, Kubota T, Manassakorn A, Ho WL, Dallorto L, Hwang YH, Kiire CA, Kuroda M, Djamel ZE, Peregrino JI, Ghosh A, Jeoung JW, Hoan TS, Srisamran N, Sandragasu T, Set SH, Doan VH, Bhattacharya SS, Ho CL, Tan DT, Sihota R, Loon SC, Mori K, Kinoshita S, Hollander AI, Qamar R, Wang YX, Teo YY, Tai ES, Hartleben-Matkin C, Lozano-Giral D, Saw SM, Cheng CY, Zenteno JC, Pang CP, Bui HT, Hee O, Craig JE, Edward DP, Yonahara M, Neto JM, Guevara-Fujita ML, Xu L, Ritch R, Liza-Sharmini AT, Wong TY, Al-Obeidan S, Do NH, Sundaresan P, Tham CC, Foster PJ, Vijaya L, Tashiro K, Vithana EN, Wang N, Aung T. Genome-wide association study identifies five new susceptibility loci for primary angle closure glaucoma. *Nat Genet.* 2016;48(5):556-562.
23. Wang S, Zhang J, Zhao A, Hipkens S, Magnuson MA, Gu G. Loss of Myt1 function partially compromises endocrine islet cell differentiation and pancreatic physiological function in the mouse. *Mech Dev.* 2007;124(11-12):898-910.
24. Hu R, Walker E, Huang C, Xu Y, Weng C, Erickson GE, Coldren A, Yang X, Brissova M, Kaverina I, Balamurugan AN, Wright CVE, Li Y, Stein R, Gu G. Myt Transcription Factors Prevent Stress-Response Gene Overactivation to Enable Postnatal Pancreatic beta Cell Proliferation, Function, and Survival. *Dev Cell.* 2020;53(4):390-405 e310.
25. Fusakio ME, Willy JA, Wang Y, Mirek ET, Al Baghdadi RJ, Adams CM, Anthony TG, Wek RC. Transcription factor ATF4 directs basal and stress-induced gene expression in the unfolded protein response and cholesterol metabolism in the liver. *Mol Biol Cell.* 2016;27(9):1536-1551.
26. Han J, Back SH, Hur J, Lin YH, Gildersleeve R, Shan J, Yuan CL, Krokowski D, Wang S, Hatzoglou M, Kilberg MS, Sartor MA, Kaufman RJ. ER-stress-induced transcriptional regulation increases protein synthesis leading to cell death. *Nat Cell Biol.* 2013;15(5):481-490.
27. Yagan MN, S.; Hu, R.; Wang, Y.; Dickerson, M., Dadi, P.; Xu, Y.; Simmons, A. J.; Stein, R.; Adams, C. M.; Jacobson, D. A.,;Lau, K.; Liu, Q.; Gu, G. . Atf4 protects islet beta-cell identity and function under acute glucose-induced stress but promotes beta-cell failure in the presence of free fatty acid. *Diabetes.* 2025;In press.
28. Quiros PM, Prado MA, Zamboni N, D'Amico D, Williams RW, Finley D, Gygi SP, Auwerx J. Multi-omics analysis identifies ATF4 as a key regulator of the mitochondrial stress response in mammals. *J Cell Biol.* 2017;216(7):2027-2045.
29. Huang C, Walker EM, Dadi PK, Hu R, Xu Y, Zhang W, Sanavia T, Mun J, Liu J, Nair GG, Tan HYA, Wang S, Magnuson MA, Stoeckert CJ, Jr., Hebrok M, Gannon M, Han W, Stein R, Jacobson DA, Gu G. Synaptotagmin 4 Regulates Pancreatic beta Cell Maturation by Modulating the Ca(2+) Sensitivity of Insulin Secretion Vesicles. *Dev Cell.* 2018;45(3):347-361 e345.
30. Walker JT, Haliyur R, Nelson HA, Ishahak M, Poffenberger G, Aramandla R, Reihsmann C, Luchsinger JR, Saunders DC, Wang P, Garcia-Ocana A, Bottino R, Agarwal A, Powers AC, Brissova M. Integrated human pseudoislet system and microfluidic platform demonstrate differences in GPCR signaling in islet cells. *JCI Insight.* 2020;5(10).

31. Petukhov V, Guo J, Baryawno N, Severe N, Scadden DT, Samsonova MG, Kharchenko PV. dropEst: pipeline for accurate estimation of molecular counts in droplet-based single-cell RNA-seq experiments. *Genome Biol.* 2018;19(1):78.
32. Butler A, Hoffman P, Smibert P, Papalexi E, Satija R. Integrating single-cell transcriptomic data across different conditions, technologies, and species. *Nat Biotechnol.* 2018;36(5):411-420.
33. Stuart T, Butler A, Hoffman P, Hafemeister C, Papalexi E, Mauck WM, 3rd, Hao Y, Stoeckius M, Smibert P, Satija R. Comprehensive Integration of Single-Cell Data. *Cell.* 2019;177(7):1888-1902 e1821.
34. Sherman BT, Hao M, Qiu J, Jiao X, Baseler MW, Lane HC, Imamichi T, Chang W. DAVID: a web server for functional enrichment analysis and functional annotation of gene lists (2021 update). *Nucleic Acids Res.* 2022;50(W1):W216-W221.
35. Sanavia T, Huang C, Manduchi E, Xu Y, Dadi PK, Potter LA, Jacobson DA, Di Camillo B, Magnuson MA, Stoeckert CJ, Jr., Gu G. Temporal Transcriptome Analysis Reveals Dynamic Gene Expression Patterns Driving beta-Cell Maturation. *Front Cell Dev Biol.* 2021;9:648791.
36. Tong X, Stein R. Lipid Droplets Protect Human beta-Cells From Lipotoxicity-Induced Stress and Cell Identity Changes. *Diabetes.* 2021;70(11):2595-2607.
37. Islam S, Zeisel A, Joost S, La Manno G, Zajac P, Kasper M, Lonnerberg P, Linnarsson S. Quantitative single-cell RNA-seq with unique molecular identifiers. *Nat Methods.* 2014;11(2):163-166.
38. Yang C, Loehn M, Jurczyk A, Przewozniak N, Leehy L, Herrera PL, Shultz LD, Greiner DL, Harlan DM, Bortell R. Lixisenatide accelerates restoration of normoglycemia and improves human beta-cell function and survival in diabetic immunodeficient NOD-scid IL-2rg(null) RIP-DTR mice engrafted with human islets. *Diabetes Metab Syndr Obes.* 2015;8:387-398.
39. Dai C, Kayton NS, Shostak A, Poffenberger G, Cyphert HA, Aramandla R, Thompson C, Papagiannis IG, Emfinger C, Shiota M, Stafford JM, Greiner DL, Herrera PL, Shultz LD, Stein R, Powers AC. Stress-impaired transcription factor expression and insulin secretion in transplanted human islets. *J Clin Invest.* 2016;126(5):1857-1870.
40. Takii R, Fujimoto M, Tan K, Takaki E, Hayashida N, Nakato R, Shirahige K, Nakai A. ATF1 modulates the heat shock response by regulating the stress-inducible heat shock factor 1 transcription complex. *Mol Cell Biol.* 2015;35(1):11-25.
41. Maekawa T, Liu B, Liu Y, Yoshida K, Muratani M, Chatton B, Ishii S. Stress-induced and ATF7-dependent epigenetic change influences cellular senescence. *Genes Cells.* 2019;24(9):627-635.
42. Levine B, Kroemer G. Biological Functions of Autophagy Genes: A Disease Perspective. *Cell.* 2019;176(1-2):11-42.
43. Neitemeier S, Jelinek A, Laino V, Hoffmann L, Eisenbach I, Eying R, Ganjam GK, Dolga AM, Oppermann S, Culmsee C. BID links ferroptosis to mitochondrial cell death pathways. *Redox Biol.* 2017;12:558-570.
44. Liadis N, Murakami K, Eweida M, Elford AR, Sheu L, Gaisano HY, Hakem R, Ohashi PS, Woo M. Caspase-3-dependent beta-cell apoptosis in the initiation of autoimmune diabetes mellitus. *Mol Cell Biol.* 2005;25(9):3620-3629.



45. Alcivar A, Hu S, Tang J, Yang X. DEDD and DEDD2 associate with caspase-8/10 and signal cell death. *Oncogene*. 2003;22(2):291-297.
46. Xu X, Xuan X, Zhang J, Xu H, Yang X, Zhang L, Zhao Y, Xu H, Li D. PSMD7 downregulation suppresses lung cancer progression by regulating the p53 pathway. *J Cancer*. 2021;12(16):4945-4957.
47. Yu CJ, Lee FJ. Multiple activities of Arl1 GTPase in the trans-Golgi network. *J Cell Sci*. 2017;130(10):1691-1699.
48. Cataldo LR, Vishnu N, Singh T, Bertonnier-Brouty L, Bsharat S, Luan C, Renstrom E, Prasad RB, Fex M, Mulder H, Artner I. The MafA-target gene PPP1R1A regulates GLP1R-mediated amplification of glucose-stimulated insulin secretion in beta-cells. *Metabolism*. 2021;118:154734.
49. Wang S, Tanaka Y, Xu Y, Takeda S, Hirokawa N. KIF3B promotes a PI3K signaling gradient causing changes in a Shh protein gradient and suppressing polydactyly in mice. *Dev Cell*. 2022;57(19):2273-2289 e2211.
50. Polgar J, Reed GL. A critical role for N-ethylmaleimide-sensitive fusion protein (NSF) in platelet granule secretion. *Blood*. 1999;94(4):1313-1318.
51. Xiao Y, Wang G, He G, Qin W, Shi Y. Rab8a/SNARE complex activation promotes vesicle anchoring and transport in spinal astrocytes to drive neuropathic pain. *Biomol Biomed*. 2024;24(5):1290-1300.
52. Li WR, Wang YL, Li C, Gao P, Zhang FF, Hu M, Li JC, Zhang S, Li R, Zhang CX. Synaptotagmin-11 inhibits spontaneous neurotransmission through vti1a. *J Neurochem*. 2021;159(4):729-741.
53. Pillon NJ, Loos RJF, Marshall SM, Zierath JR. Metabolic consequences of obesity and type 2 diabetes: Balancing genes and environment for personalized care. *Cell*. 2021;184(6):1530-1544.
54. Henry C, Close AF, Buteau J. A critical role for the neural zinc factor ST18 in pancreatic beta-cell apoptosis. *J Biol Chem*. 2014;289(12):8413-8419.
55. Yang J, Siqueira MF, Behl Y, Alikhani M, Graves DT. The transcription factor ST18 regulates proapoptotic and proinflammatory gene expression in fibroblasts. *FASEB J*. 2008;22(11):3956-3967.
56. Lee J, Taylor CA, Barnes KM, Shen A, Stewart EV, Chen A, Xiang YK, Bao Z, Shen K. A Myt1 family transcription factor defines neuronal fate by repressing non-neuronal genes. *Elife*. 2019;8.
57. Vasconcelos FF, Sessa A, Laranjeira C, Raposo A, Teixeira V, Hagey DW, Tomaz DM, Muhr J, Broccoli V, Castro DS. MyT1 Counteracts the Neural Progenitor Program to Promote Vertebrate Neurogenesis. *Cell Rep*. 2016;17(2):469-483.
58. Tong X, Yagan M, Hu R, Nevills S, Doss TD, Stein RW, Balamurugan AN, Gu G. Metabolic Stress Levels Influence the Ability of Myelin Transcription Factors to Regulate beta-Cell Identity and Survival. *Diabetes*. 2024;73(10):1662-1672.